

It is thus evident that the low critical Reynolds number is due to the turbulence level in the tunnel.

### 8.3 LIFT VARIATION WITH SPIN PARAMETER

Due to the difficulty experienced in obtaining literature, certain assumptions made at the outset of this experimental work were not always based on a complete knowledge of the available material. The first assumption made was that since the Lift curve published by Davies (1949) and the one published in Tritton (1979) (quoting Maccoll) were both for Reynolds numbers of 100 000 and showed the same profile with minor deviations, this was a valid curve for a spinning sphere. It was also assumed that these were the only tests published by either of the experimenters. Later a copy of Maccoll's paper (1928) was obtained and it was found that he had published the results of five tests up to a Reynolds number of 109 000. A third order polynomial could be fitted to the results of both Davies and Maccoll. The accuracy of this fit could well be ascribed to experimental error. For this reason it was decided to assume that a third order polynomial was the trend of the Lift and Drag curves.

The first series of tests displaying the results of Lift versus spin parameter or velocity ratio was carried out with the original aluminium uprights in the parallelogram support system (Fig. 7.18). The support did move visibly but this was not due to imbalance of the sphere since if the wind tunnel was switched off the support did not move while the sphere was spinning. The individual tests are displayed in Fig. 7.5 to Fig. 7.10 and then displayed on a single pair of axes in Fig. 7.19.

The first test in this series was carried out at a Reynolds number of 70 000 (Fig. 7.5). Although the coefficient of lift did not increase linearly with spin parameter, as expected because of the theory in section 5.1, it did increase. Although the theory quoted in section 5.1 is for a cylinder it was thought to be acceptable as a first approximation. After comparing the results of the present work with those of Swanson (1961) it is evident that the behaviour of a sphere and a cylinder are very similar. The lack of linearity could be ascribed to the fact that as the spin parameter increases the shear effects increase thus rendering a potential flow approximation inaccurate.

When the Reynolds number was increased to 138 000 the Lift fluctuated about the zero line between a spin parameter of 0.2 and 0.6 (Fig. 7.6). From a Reynolds number of 188 000 upward the Lift went through a negative region before going positive and was more stable. The minimum point seemed to increase in magnitude with increased Reynolds number.

The above tests showed tendencies not previously mentioned in the literature on spinning spheres referred to by the Author. The first noticeable difference was that the minimum Lift achieved by both Davies and Maccoll was approximately -0.1, whereas the present results showed that the minimum Lift could reach -0.6. Another noticeable deviation from Davies and Maccoll was that the minimum Lift would increase in magnitude with increasing Reynolds number. The third obvious deviation was that the Lift went through zero at a velocity ratio of 0.4 according to Davies and 0.44 according to Maccoll and in the region of 0.6 in the present tests. To investigate this further it was decided that during the next series of tests, a test would be run at a Reynolds number of 95 000 which is in the region of both the tests carried out by Davies and Maccoll.

The tests were repeated using the same support with stainless steel uprights and the sting rotated through 90° about its longitudinal axis. The uprights were replaced to increase the stiffness. It was thought that the lack of stiffness was the cause of fluctuation in the Reynolds number range of 135 000 and 155 000. The sting was rotated to move a faulty component to a position where it would have minimal influence on the results of Lift and Drag.

These results are given individually in Fig. 7.11 to Fig. 7.14, and the last two tests combined on a common pair of axes in Fig. 7.19.

The first test in the second series was carried out at a Reynolds number of 95 000 to allow for comparison with the results of Davies and Maccoll who carried out tests in this region. The results of the tests carried out by both Davies and Maccoll are given in Chapter 3, Fig 3.8 to Fig. 3.21. These results were taken from their original papers and do not rely on any other sources to limit errors. There are a few assumptions made to be able to give these results in the same format as the results from the present tests and if other sources are quoted their respective assumptions cannot be checked as they have not been stated. The first assumption is that the error due to photostating graphs is negligible as the resulting error will be reasonably uniform. The results quoted from Davies state that he got a  $C_D = 0.44$  for the first test with no spin and from this it was possible to calculate the density of that test. It was then assumed that the density was constant for all his tests. For Maccoll's results it was assumed that the Sea Level conditions applied for the

calculation of Reynolds number. These assumptions will not lead to a significant error and were essential to convert the published results to those used in this report.

The Lift curve followed that of Davies until a velocity ratio of 0.2 and then fluctuation set in. This fluctuation was purely due to aerodynamic effects as the sphere showed no tendency to hit natural frequency when spun without the wind tunnel switched on. The minimum Lift value obtained in this test corresponded to that of Davies before the fluctuation set in but there appeared to be three cross over points.

From Fig. 7.11 and Fig. 7.12 it appears that the unstable region was larger than that evident in previous tests and ranged from 95 000 to 155 000. The tendency of the minimum Lift increasing in magnitude with increasing Reynolds number is also evident in the last two tests in this series. The cross over point occurred in the region of 0.6 and the minimum Lift was of the order of -0.6 for a Reynolds number of 230 000.

A third series of tests was carried out using a solid support to try to damp out the unstable region. These results are displayed in Fig. 7.15 to Fig. 7.17 individually and the tests without fluctuation are displayed on common axes in Fig. 7.20. The results in Fig. 7.17 show the general trend that the other tests display but the minimum Lift value only reached approximately -0.4 instead of approximately -0.6. Disregarding this test from the series meant that the trend of increased magnitude of minimum Lift with increasing Reynolds number could not be verified. The cross over point was still in the region of a velocity ratio of 0.6. The test carried out at a Reynolds number of 165 000 (Fig. 7.15) showed a tendency to fluctuate yet remained in the negative range. The fluctuation between a spin parameter of 0.65 and 1 is not found in any other test results. This fluctuation is thought to be due to the vortex shedding frequency and rotational frequency combination exciting a natural frequency of the model and support B assembly, when the spin parameter was in the range 0.65 and 1.

The explanation given by Davies for the negative lift was that although the resultant velocity is higher on the one side than on the other, the flow on either side does not necessarily possess the same quality. If one examines the flow over a stationary sphere, at low velocities the flow follows the surface of the sphere. As the velocity increases the flow separates and forms a wake. As the velocity increases still further, the point of separation moves towards

the front of the sphere until the boundary layer becomes turbulent. Once the flow is turbulent the separation point moves towards the back of the sphere again. This results in the pressure profile shown below.

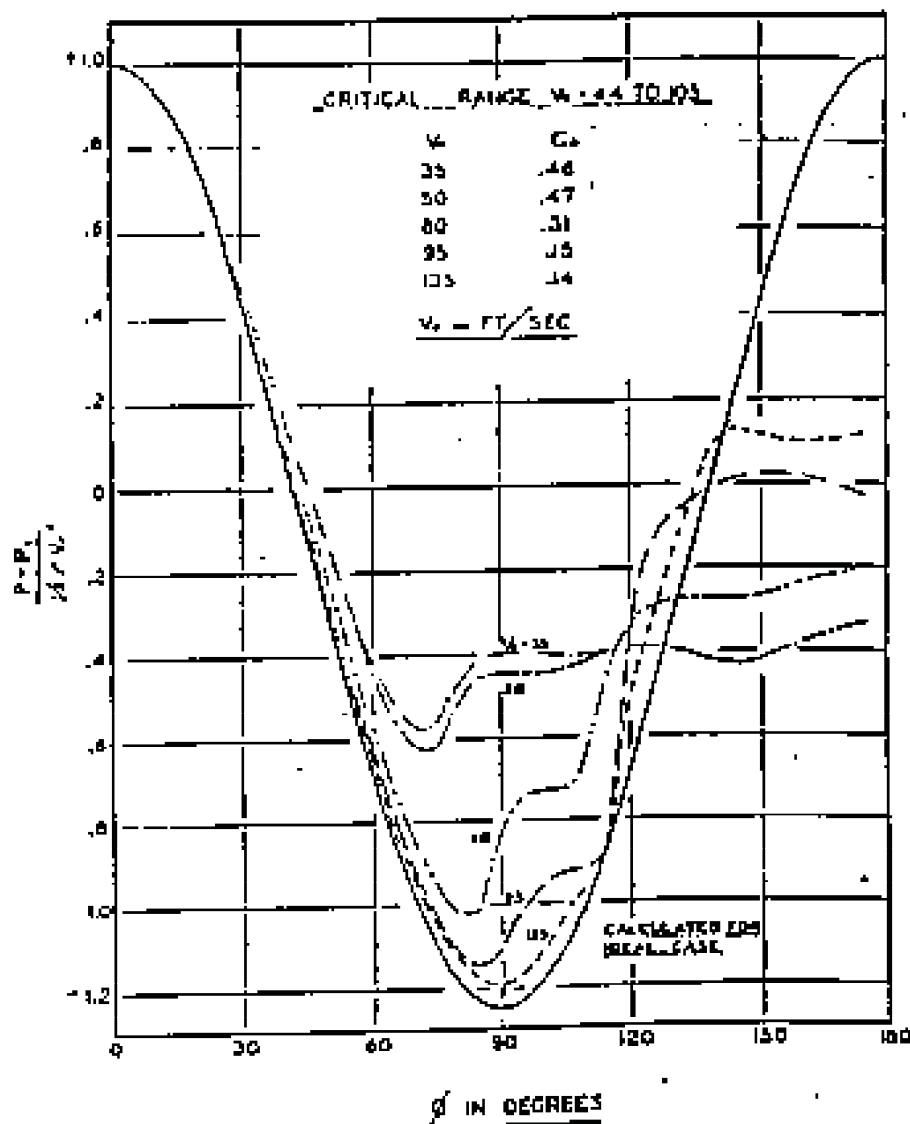


Fig 8.1 Pressure distribution over a stationary sphere. (FAGE)

The sphere when it is spinning could have one surface with a relative velocity of 35 ft/s at (a) and the other 135 ft/s at (b). Based on this the pressure at (b) is lower than the pressure at (a) resulting in a negative lift.

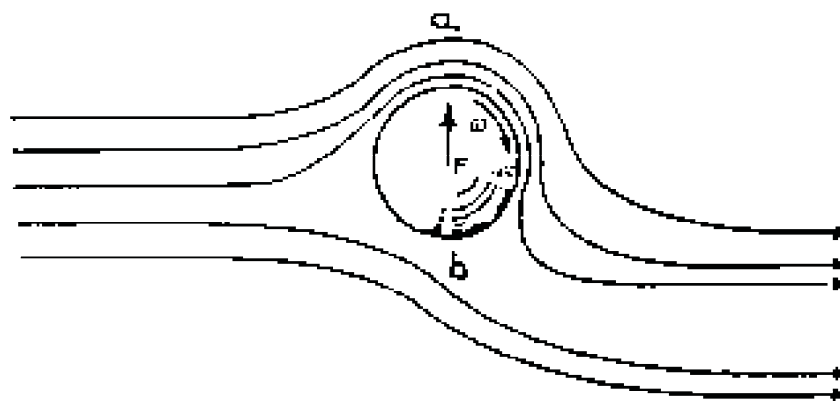


Fig. 8.2 Flow over a rotating sphere with axis of spin perpendicular to the wind axis.

Davies performed his tests at a Reynolds number of 90 000 and Maccoll performed his tests between  $Re = 32\ 000$  and  $Re = 109\ 000$ . Maccoll achieved a velocity ratio of 7 when testing at low Reynolds numbers but when the wind velocity increased the maximum velocity ratio dropped since the maximum angular velocity of the sphere had been reached. He also had problems with minimum angular velocity and probably incrementing the angular velocity as he could only pick up one point in the negative lift region at a Reynolds number of 79 000 and two at a Reynolds number of 109 000.

Swanson (1961) used the same logic to explain the negative lift region experienced by a spinning sphere. The similarities in behaviour of the Lift coefficient with Spin parameter are very noticeable.

One has to consider the whole experimental system and all its variables before making any conclusions. The three experimenters used three totally different sets of apparatus and three different model sizes. The Author used three separate support systems to determine the effect this would have on the results and found that the effect was minimal. The quality of flow in the tunnel certainly has an effect on the results. According to Dryden this would just shift the effective Reynolds number up by the turbulence factor. The turbulence factor for the tunnels used by both Davies and Maccoll is not known. Another variable that can affect the results is the model size. In an attempt to eliminate this effect Maccoll and the Author used nondimensionalization based on density, velocity squared and the diameter squared.

This is standard for aerofoils but the Author has found no experimental justification for this pertaining to spheres. This leaves the only justification being dimensional analysis.

If the results of all the present tests are considered together, then the behaviour of the spinning sphere can be divided into three categories. The first category is that for a Reynolds number of up to 70 000. The second region is that between 95 000 and 165 000 and the third region is that from 188 000 to 250 000. The first region does not develop negative lift. The lift increases and then levels off. The level region is not flat but does show a tendency to fluctuate gently. This observation appears to be independent of model size or wind tunnel and support system.

The second region shows a tendency to fluctuate. If this fluctuation is effectively a slow oscillation and the averaging system used in the present tests does not cover a long enough period, then this would explain why neither Davies nor Maccoll mentioned it. Davies calculated the Lift and Drag from the displacement of his sphere when dropped into the wind tunnel. He would therefore be averaging his forces for the entire flight. Maccoll on the other hand used a mechanical system to measure his forces and no indication of the damping effects was given. The readings were also taken by the experimenter reading the value off a scale which would automatically average the results over a fairly long period.

The results of the present tests are based on averaging. The UPM 60 averages the signal for 20 ms before scanning the next channel. This is carried out for a number of cycles and the average of each channel is then used as the final data. The lift on a cylinder shedding turbulent vortices oscillates (Gerrard 1961). Compound this problem with spin and the behaviour of the vortices can not be assumed to be steady.

The third region displays much more steady results and a definite negative lift region. There is however a slight fluctuation of the point at which the lift becomes positive. This is in the region of a velocity ratio of 0.6. Davies obtained a cross over point at a velocity ratio of approximately 0.38 and Maccoll's cross over point occurred at approximately 0.44. This discrepancy could be due to the wind tunnel turbulence and atmospheric conditions. The Author does not consider the size of model to be the cause of this discrepancy as the size difference between Davies and Maccoll is much larger than

that between Maccoll and the present model and yet the difference between the results of Davies and Maccoll is smaller than that between Maccoll and the present tests.

The point of maximum negative Lift was in the region of  $A = 0.2$ . This could not be verified by the tests carried out by Maccoll but those carried out by Davies showed a "minimum" at this point when a third order polynomial was fitted to the data (Fig. 3.18 & Fig. 3.19).

Justification for splitting the tests into three ranges was difficult to find, but eventually a paper by Swanson (1961) was located. Although he was testing a spinning cylinder, he also used electronic transducers to measure his loads. His cylinder had a six inch diameter and he also experienced fluctuation in his results at similar Reynolds numbers. The lowest Reynolds number region where Swanson found a cross over indicating fluctuation was between  $Re = 90\,000$  and  $Re = 128\,000$  (Fig. 3.2 & Fig. 3.3). He also found that the smooth curve of lift variation with spin parameter occurred between  $Re = 181\,500$  and  $Re = 360\,000$ . Swanson also stated that for a cylinder the lift force fluctuations could vary in magnitude by an amount of the same order as the average value of the net force. He attributes this to the random fluctuating wake pressure and velocity field which are then propagated throughout the entire flow field. The graphs in Fig. 3.2 and Fig. 3.3 also show that the change over from negative to positive Lift occurred between a spin parameter of  $A = 0.5$  to  $A = 0.6$ . The maximum negative lift increased with Reynolds number up to a Reynolds number of  $360\,000$  and then started to decrease. This is consistent with the results of the present experimentation on spheres, as testing was only carried out to a Reynolds number of  $250\,000$ . The maximum negative Lift measured by Swanson was also close to  $C_L = -0.6$ .



#### **8.4 DRAG VARIATION WITH SPIN PARAMETER**

The results of the first set of tests (Fig. 7.21 to Fig. 7.24) compared with Davies results (Fig. 3.20) and Fig. 3.21) exceptionally well. There was no evidence of a sharp drop in Drag value as can be seen in the test using support A in position 2 at a high Reynolds number of 230 000 (Fig. 7.26).

The sharp drop in Drag would indicate transition although it does not drop far below a  $C_D$  of 0.3 but oscillates about this value. This would imply that spin can induce transition but would not always do so. The Author is of the opinion that whether spin would induce transition or not is not based on the steady phenomenon alone and would therefore be a result of many influences not covered in this study.

The tests carried out using support B in position 2 (Fig. 7.27 and Fig. 7.28) showed the same slow oscillation that is evident in all the tests on spinning spheres, including those carried out by Davies and Maccoll. The fact that both these tests had a drag coefficient of 0.2 for the no spin condition implies that the test was carried out above the critical Reynolds number. The test of drag variation with Reynolds number using support B (Fig. 7.4) showed that the Drag coefficient did drop at  $Re = 225\ 000$ , but was not sufficient to call critical. This test however, was carried out with the sting axis parallel to the wind axis. No Drag variation with Reynolds number testing was carried out using this support with the spin axis perpendicular to the wind axis. It is therefore possible that these tests were carried out at a Reynolds number above critical; as there is no conclusive proof, no conclusions can be drawn from the results in Fig. 7.27 and Fig. 7.28.

### **8.5 PREDICTION OF LIFT VARIATION WITH YAW**

It is known that spin perpendicular to the wind axis results in Lift on the sphere. What is not documented is the Lift generated when the spin axis is not perpendicular to the wind. The prediction of Lift variation with yaw is usually based on the assumption that the spin can be considered a vector and therefore broken down into component vectors. The component of spin is therefore calculated along the axis perpendicular to the wind. The Lift value for this spin parameter is then used as the predicted Lift for the given angle. To give a smoother curve a third order polynomial was fitted to the data of three tests already carried out and a predicted Lift variation of Yaw was calculated for each.

The third order polynomial was fitted by means of a least squares approximation given in the theory section (Chapter 5.5). The resulting equations are given in the results section with a graph showing the fitted equation compared to the experimental data (Chapter 7.6.1) and the predicted curves for each case (Chapter 7.6.2).

Three particular cases were considered to give an example in each of the three regions mentioned in the section covering lift developed due to spin perpendicular to the wind axis. The cases considered were:

$Re = 70\,000$	$A = 0.6$
$Re = 165\,000$	$A = 0.95$
$Re = 230\,000$	$A = 0.6$

The results of the above predictions are compared with experimental tests in the next section. This method would verify whether the assumption that spin, defined as a vector, can be broken down into component vectors, is valid or not.

## 8.6 LIFT AND DRAG VARIATION WITH YAW ANGLE

The results of the Lift variation with Yaw angle will be discussed first and then the variation of Drag with Yaw angle will be considered. When designing aerodynamic objects the first concern is the Lift produced and then one considers the Drag that has to be overcome.

The result of assuming that spin is a vector and can be broken into components, an assumption commonly used in physics, showed that as the angle of Yaw was increased from  $0^\circ$  to  $90^\circ$  the Lift would follow the curve of Lift variation with increased velocity ratio up to the velocity ratio that the sphere is operating at for the test in question. For this reason the tests were carried out with the sphere spinning at the maximum rotational velocity possible. Using a lower rotational velocity might not have given measurable changes in force.

Irrespective of the support used or the position of the sting during testing the Lift variation with Yaw angle did not support the assumption that the spin could be broken into component vectors. The general trend was a large increase to start with and then a levelling off, with a slight upward trend right at the end. Those tests carried out after the repair of the sting (Fig. 7.42, Fig. 7.43 & Fig. 7.44) showed the same general trend but gave a much smoother set of results than any previously obtained. The Author is of the opinion that these are the best reflection of the variation of Lift with Yaw angle from the present research.

The variation of Drag with velocity ratio did show a repeatable trend of oscillation within given bounds but the maxima and minima were not at given velocity ratios. Since the bounds were relatively close the correlation between expected and experimental results was not expected to be very good.

The change in Yaw angle can cause the onset of transition or the reversion to laminar flow results. In Fig. 7.29 the change in angle from zero to  $10^\circ$  resulted in a significant drop in Drag from  $C_D = 0.5$  to  $C_D = 0.3$ . The drag value tends to fluctuate about the 0.3 level thereafter. In Fig. 7.30 the Drag had a tendency to increase with increased Yaw angle. The results in Fig. 7.31 showed both the ability to cause a drop in Drag and the ability to revert to a high Drag value. The results in Fig. 7.32 confirmed those in Fig. 7.29. Fig. 7.33 showed the phenomenon of reversion from turbulent to laminar Drag values. Fig. 7.34 however just showed the tendency to increase slightly to a  $C_D = 0.3$  and then fluctuate about this value.

The change in Yaw angle both for  $\gamma$  close to  $0^\circ$  and  $\gamma$  close to  $90^\circ$  can result in the onset of transition. From the present tests it cannot be established that spin can be assumed to behave like a vector and be broken down into component vectors throughout the range of Yaw, but both the resulting transition and reversion to laminar Drag values could be the result of this assumption being valid for small angles.

### **8.7 RELATIONSHIP OF DRAG TO SPIN PARAMETER FOR SPIN PARALLEL TO THE FLOW**

This test was also carried out with both support systems and both orientations of the sting. The Drag seemed to be influenced by the spin parameter but the influence was not repeatable. This may have been due to the low rate of data acquisition. What was evident was that the spin had an effect on transition. Schlichting shows that spin has an effect on the critical Reynolds number. For the range  $A = 0$  to  $A = 1$  transition is retarded.

The present tests show that spin causes the Drag to fluctuate. Below a Reynolds number of approximately 200 000 there is a fluctuation but no sharp drops. The test carried out at  $Re = 200\ 000$ , the Drag value dropped sharply at  $A = 0.5$  but did not remain low. It fluctuated implying that transition was not complete. For Reynolds numbers in the region of 240 000 to 250 000 the spin did show the ability to induce transition if this had not set in already.

It can be stated that spin parallel to the wind axis can induce transition for Reynolds numbers above 200 000 but further testing would be required to understand when and how this occurs.

## 8.8 RECOMMENDATIONS

To give an indication of the turbulence levels present in the wind tunnel, It is recommend that a smaller sphere be used to determine the critical Reynolds number of a stationary sphere in this particular tunnel. The results can be manipulated according to Dryden's method as quoted by Rae and Pope (1984).

If the research on spinning spheres were to be continued then I would recommend that the UPM 60 be removed from the system as the digital to analogue converter, as it is too slow. This would mean that the data being read could give an idea of the fluctuation in forces due to vortex shedding.

I would recommend that the test duration be lengthened to facilitate the valuation of large period mean values, while using a faster data acquisition system to be able to obtain measurements of the fluctuations in force during the same test.

I would also recommend that the support system be analysed so that a more satisfactory unit could replace it. When using rotating models or models shedding vortices, the excitation frequency must not be anywhere near the natural frequency of the support and model unit. With all three support systems the sphere could not be tested at a particular velocity and spin rate combination dependant on the support used. A proper design would be an involved problem as the floor vibrates, there are space limitations and flow interference must be kept to a minimum.

## 9 CONCLUSIONS

The tests monitoring the relationship of Drag to Reynolds number, showed that the mean values were within the band set by the published data. The results did have fluctuations which were dependant on the stiffness of the support.

A conservative estimate of the turbulence level is 0.65.

The Lift variation with velocity ratio can be divided into three ranges

1. For  $Re \leq 70\ 000$  no negative lift is generated but positive Lift is generated. The Lift tends towards a maximum value and then levels off.
2. For  $95\ 000 \leq Re \leq 165\ 000$  negative Lift was generated but a fluctuation was also evident.
3. For  $188\ 000 \leq Re \leq 250\ 000$  negative Lift was generated and no major fluctuation was evident.

The negative Lift tends to increase with increasing Reynolds number.

The maximum negative Lift was of the order of -0.6.

The maximum negative Lift occurred in the region of  $A = 0.2$ .

The effect of spin perpendicular to the wind in the present set of tests correlated with those published both by Davies and Maccoll. It seems apparent that spin perpendicular to the wind axis can induce transition when testing in the critical Reynolds number range.

The present experimental results do not validate the assumption that the spin can be regarded as a vector and split into components throughout the range of  $0^\circ$  to  $90^\circ$ .

The effect of spin can induce transition when the spin is either perpendicular or parallel to the wind axis.

It is clear, both from the literature survey and current tests that the flow around a spinning sphere is highly complex, considerably more so than for a cylinder, which is in itself not fully understood. Unsteady boundary layer and wake effects would require careful study in order to explain some of the effects reported in this dissertation.

## 10 REFERENCES

- ACHENBACH E., Experiments on the Flow Past Spheres at very High Reynolds Numbers, *J. Fluid Mech.*, 54, pp.565-575 (1972)
- ACHENBACH E., Vortex Shedding from Spheres, *J. Fluid Mech.*, 62, pp.209-221 (1974)
- ALDOSS T.K. and MANSOUR A., Theoretical calculation of the flow around a Rotating Circular Cylinder Placed in a Uniform Flow, *Transactions of ASME*, 110, pp.96-98 (1988)
- ANDERSON J.D., *Fundamentals of Aerodynamics*, Mc Graw-Hill, 1984
- BARKLA H.M. and AUCHTERLONIE L.J., The Magnus or Robbins effect on rotating spheres, *J. Fluid Mech.* (1971), 47, pp.437-447
- BEARMAN P.W. and HARVEY J.K., Golf Ball Aerodynamics, *Aeronautical Quarterly*, May 1976, pp.112-122
- CALVERT J.R., Some Experiments on the Flow Past a Sphere, *Aero. J. Roy. Aern. Soc.* 76, pp.248-250 (1972)
- COMETTA C., An Investigation of the Unsteady Flow Pattern in the Wake of Cylinders and Spheres using a Hot-Wire Probe, Division of Engineering, Brown University, Technical Report WT-21 (1957)
- DAVIES J.M., The Aerodynamics of golf balls. *J. of Applied Physics*, 20 No 9, 821 (1949)
- ESMAIL M.N, HUMMEL R.L. and SMITH J.W., Notes on Experimental Velocity Profiles in Laminar Flow around Spheres at Intermediate Reynolds Numbers, *J. Fluid Mech.*, 90, pp.755-799 (1979)
- GERRARD J.H., An Experimental Investigation of the Oscillating Lift and Drag of a Cylinder Shedding Turbulent Vortices, *J. Fluid Mech.*, 11, pp.244-256 (1961)
- HAMMELER A.E., STOREY S.H. and WHITEHEAD J.M. Viscous Flow Around Fluid Spheres at Intermediate Reynolds Numbers (II). *Can. J. Chem. Eng.*, 41, 246 (1963)



- HAMIELEC A.E., HOFFMAN T.W., and ROSS L.L. Numerical Solution of the Navier-Stokes Equation for Flow Past Spheres Part I "Viscous flows around spheres with and without radial mass efflux. A.I.Ch.E. Journal, 13 No 2, 212 (1967)
- HAMIELEC A.E., JOHNSON A.I and HOUGHTON W.T. Numerical Solution of the Navier-Stokes Equation for Flow Past Spheres Part II "Viscous flows around circulating spheres of low viscosity. A.I.Ch.E. Journal, 13 No 2, 220 (1967)
- HOUGHTON E.L., and CARRUTHERS N.B., Aerodynamics for Engineering Students, third edition, Edward Arnold (1982)
- HORLOCK J.H., The Swing of a Cricket Ball, Cambridge University Mechanical Engineering Department (1973)
- KIMURA T. and TSUTAHARA M., Flows about a Rotating Circular Cylinder by the Discrete Vortex Method, AIAA JANUARY (1987)
- MACCOLL J.W., Aerodynamics of a spinning sphere, J. Roy. Aeronautical Soc., 32, pp.777-798 (1928)
- MASSEY B.S., Mechanics of fluids, Van Nostrand Reinhold (International) London, 4 edition (1979)
- MAXWORTHY T., The Flow Created by a Sphere Moving Along the Axis of a Rotating, Slightly-Viscous Fluid, J. Fluid Mech., 40, pp.453-479 (1970)
- Mc CORMICK B.W., Aerodynamics of V/STOL Flight, Academic press 1967
- MEHTA R.D., Aerodynamics Of Sports Balls, Ann. Rev. Fluid Mech., 17, pp.151-189 (1985)
- PAO H. and KAO T.W., Vortex Structures in the Wake of a Sphere, The Phys. of Fluids, 20, No 2, pp.187-191 (1977)
- PRUPPACHER H.R., LE CLAIR B.P. and HAMIELEC A.E., Some relations between Drag and Flow Pattern of Viscous Flow Past a Sphere and a Cylinder at Low and Intermediate Reynolds Numbers, J. Fluid Mech, 44, pp.781-790 (1970)
- RAE W.H. and POPE A., Low Speed Wind Tunnel Testing, second edition, John Wiley & Sons 1984

- RAYLEIGH Lord, On The Irregular Flight Of A Tennis Ball, Messenger of mathematics, 7, 14 (1877)
- ROUSE H., Elementary Mechanics of Fluids, John Wiley & Sons 1946
- RUBINOW S.I. and KELLER J.B., The Transverse Force on a Spinning Sphere Moving in a Viscous Fluid, J. Fluid Mech. 11, 447 (1961)
- SARPKAYA T. and SCHOAFF R.L., Inviscid model of Two-Dimensional Vortex Shedding by a Circular cylinder, AIAA Journal, 17, pp.1193-1200 (1979)
- SCHLICHTING H., Boundary-layer theory, seventh edition, Mc Graw-Hill, 1979
- SEELEY L.E., HUMMEL R.L. and SMITH J.W., Experimental Velocity Profiles in Laminar Flow around Spheres at Intermediate Reynolds Numbers, J. Fluid Mech, 68, pp.591-608 (1975)
- SINGH S.N., The Flow Past a Spinning Sphere in a Slowly Rotating Fluid at Small Reynolds Number, Int. J. Eng. Sci., 13, pp.1085-1089, (1975)
- SWANSON W.M., The Magnus Effect: A Summary of the investigations to date, Transactions of ASME, pp.461-470 (Sept 1961)
- TANEDA S., Studies on Wake Vortices III, Experimental Investigation of the Wake Behind a Sphere at Low Reynolds Numbers, J. Phys. Soc. Japan, 11, 302 (1956)
- TANEDA S., Visual Observations of the flow Past a Sphere at Reynolds Numbers between  $10^4$  and  $10^6$ , J. Fluid Mech, 85, pp.187-192 (1978)
- TRITTON D.J., Physical Fluid Dynamics, Van Nostrand Reinhold, 1979
- VAN DYKE M., Perturbation methods in Fluid Mechanics, Academic press 1964
- ZAPRYANOV Z., Boundary Layer Growth on a Spinning Sphere, Z Angew. Math. & Mech., 57, No 1, pp.41-46 (Jan 1977)

## **APPENDIX A**

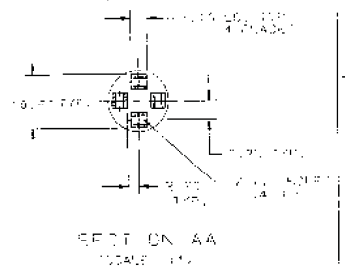
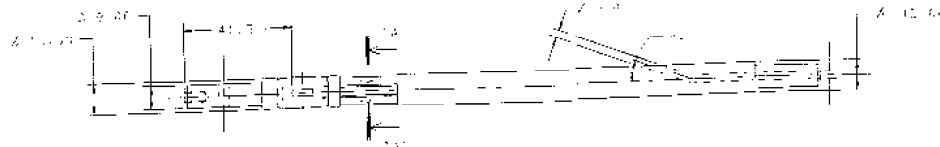
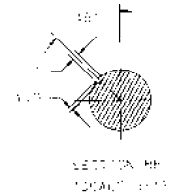
### **DESIGN OF BALANCE SYSTEM**

#### **DESIGN OF 12mm STING BALANCE**

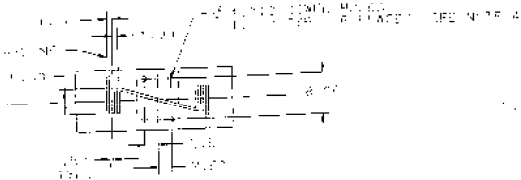
The design of the sting balance was contracted out to DAST of the CSIR to design, build and calibrate. The general theory is described in the main body of this report. A technical drawing is inserted at the end of this section.

The sting has still got a problem with the Y component but will be sent back for repairs as soon as this set of tests has been completed.

The sting did not come with any documentation other than a calibration matrix. The calibration was done using  $\beta$  factors but the formulae were not supplied. The resistors supplied were not those used in the calibration either. The theory supplied in this report is that which was used for the calibration and operation during testing and is similar to that used by DAST as far as I can ascertain.

[illegible]

1	2	3	4	5	6	7	8	9	10	11	12	13	14	15	16	17	18	19	20	21	22	23	24	25	26	27	28	29	30	31	32	33	34	35	36	37	38	39	40	41	42	43	44	45	46	47	48	49	50	51	52	53	54	55	56	57	58	59	60	61	62	63	64	65	66	67	68	69	70	71	72	73	74	75	76	77	78	79	80	81	82	83	84	85	86	87	88	89	90	91	92	93	94	95	96	97	98	99	100
1	2	3	4	5	6	7	8	9	10	11	12	13	14	15	16	17	18	19	20	21	22	23	24	25	26	27	28	29	30	31	32	33	34	35	36	37	38	39	40	41	42	43	44	45	46	47	48	49	50	51	52	53	54	55	56	57	58	59	60	61	62	63	64	65	66	67	68	69	70	71	72	73	74	75	76	77	78	79	80	81	82	83	84	85	86	87	88	89	90	91	92	93	94	95	96	97	98	99	100

$$\sigma_{\text{max}} = 1.5 \times 10^3 \text{ MPa} \quad \sigma_{\text{min}} = 1.5 \times 10^3 \text{ MPa}$$

$$\overline{D} = A \cup \{0\} \cup \{1\} \cup \{x \mid 0 \leq x \leq 1\}$$

4	1	2	3	4	5	6	7	8	9	10	11	12	13	14	15	16	17	18	19	20	21	22	23	24	25	26	27	28	29	30	31	32	33	34	35	36	37	38	39	40	41	42	43	44	45	46	47	48	49	50	51	52	53	54	55	56	57	58	59	60	61	62	63	64	65	66	67	68	69	70	71	72	73	74	75	76	77	78	79	80	81	82	83	84	85	86	87	88	89	90	91	92	93	94	95	96	97	98	99	100
1	2	3	4	5	6	7	8	9	10	11	12	13	14	15	16	17	18	19	20	21	22	23	24	25	26	27	28	29	30	31	32	33	34	35	36	37	38	39	40	41	42	43	44	45	46	47	48	49	50	51	52	53	54	55	56	57	58	59	60	61	62	63	64	65	66	67	68	69	70	71	72	73	74	75	76	77	78	79	80	81	82	83	84	85	86	87	88	89	90	91	92	93	94	95	96	97	98	99	100	

[illegible]

## DESIGN OF BALANCE SUPPORT SYSTEM

This is not a full report on the design of the balance support system as the Author did not think that it was relevant to the report as a whole. Only the main considerations and overall description are noted. A few of the extra features are mentioned in passing.

Because the sting had to be used on the spinning sphere project as well as facilitate general use for wind tunnel testing, some of the specifications *are a bit more extreme than the* conventional support found in a wind tunnel. An example of this is the Yaw limits being set at  $\pm 90^\circ$ .

The requirements set were;

- 1) The angle of Attack must range from  $-30^\circ$  to  $30^\circ$ .
- 2) The angle of Yaw must range from  $-90^\circ$  to  $90^\circ$ .
- 3) *The support must have as little effect on the model as possible.*
- 4) The model must remain in the most uniform region of the flow.
- 5) As little of the vibration transmitted to the mezzanine floor from the fan must be transmitted to the model and transducer elements.
- 6) The position of the model must be known for each test.

A turn-table was supplied with the wind tunnel *when it was received from* ESCOM. This was cut down so that any support system built could be placed on it and the support would have a Yaw capability. The bearings were replaced as they were badly *wearered*. *To prevent vibration being* transmitted up the support the turn-table was placed on shock pads.

It was decided that the best method of support for a model would be a sting. The reason for this was that the interference from a *sting is minimal*. This is because the sting is generally in the wake behind the model. The measuring elements in a sting balance are near the end of the sting resulting in minimal tare. The transformation of *measured forces and* moments to the centre of gravity of the model is also kept to a minimum.

The sting was supported by a parallelogram support. The reason for this is that the model is in the same spatial position at all angles of Yaw and Attack. This means that the model can be placed in the centre of flow which is usually the area of most uniform flow and all the tests carried out under the same conditions. The tests at the limits of angular displacement also have the same flow quality as those in the zero position and wall effects do not need to be considered. All the joints were pins with a brass bush around them to allow for minimum friction.

To speed up testing all the variables were fed into the computer for each test automatically by the UPM 60. The angles of Attack and Yaw were also required so that the position of the model would be known for each test. The angular displacement was measured by a linear potentiometer, the resistance of which varied linearly with the rotation of the control. The most sensitive method of measuring resistance changes, was using a Wheatstone bridge. Two potentiometers were connected to form a bridge so that the zero setting could be altered. The reason for this was that the bridge can only measure a fixed angular displacement from the zero position before reaching the limit of the UPM 60. The limit was less than  $90^\circ$ . By inserting a resistor in series with the bridge the range was increased to  $\pm 120^\circ$ .

The limit of angular displacement for the potentiometers used was  $270^\circ$  so stops were bolted to the underside of the table to prevent damage to the potentiometers when the turn-table was rotated. A friction brake was also fitted so that the angle of Yaw could be maintained. The limits of the angle of attack were set by the proximity of the two horizontal parallel bars. The potentiometer for the measurement of angle of attack was placed on a pin joint vertically below the model.

The angle of attack was changed by means of a wormgearbox at the lowest pin joint vertically below the model. The gearbox reduction ratio was 100 to 1 facilitating fine setting. The gearbox also acted as a break so that once the angle of attack was set the model would not move apart from the slight freeplay in the system.

The angle of Yaw could be changed by releasing the break and manually rotating the table or by using a handle connected to the table by a chain and cog system. The handle was situated near the computer to make it easier to change the angle of Yaw from the computer area.

A disk was cut out of the floor of the test section to facilitate the sting support. The disk was then mounted on the top of the turn-table with a slot cut out, to allow the vertical uprights to pass into the flow. The disk then prevented external flows from entering through the hole in the floor. The disk was spring mounted so that the floor of the tunnel would be as flush as possible.

All the requirements originally set out were met to the best of our ability. However there remain a few problems with the support. I would suggest that the support be made stiffer and the freeplay be reduced as much as possible. It is also suggested that the circuit used to measure the angular displacement be designed to operate at an optimum level and not just functionally.

## APPENDIX B

Output from multiple linear regression carried out by STATGRAPHICS on the calibration results of the sting in position 1.

Model fitting results for: D:CALDCJ.XFORCE

```
*****
Independent variable      coefficient std. error   t-value  sig.level
*****
D:CALDCJ.BETA1           -0.043029  0.000298  -144.5813  0.0000
D:CALDCJ.BETA2           -0.000107  0.000232   -0.4613   0.6447
D:CALDCJ.BETA3            0.001265  0.000272    4.6502   0.0000
D:CALDCJ.BETA4            0.001118  0.00161    0.6944   0.4877
D:CALDCJ.BETA5            0.000078  0.000349    1.0275   0.3046
D:CALDCJ.BETA6           -0.010341  0.000879  -11.7666   0.0000
*****

R-SQ. (ADJ.) = 0.9743  SE = 0.477205  MAE = 0.293341  DurbWat = 0.156
552 observations fitted for 0 missing val. of dep. var.
```

### Output for regression of the X force versus $\beta$

Model fitting results for: D:CALDCJ.YFORCE

```
*****
Independent variable      coefficient std. error   t-value  sig.level
*****
D:CALDCJ.BETA1            0.000163  0.000088    1.8455   0.0655
D:CALDCJ.BETA2            0.005393  0.000069   78.5448   0.0000
D:CALDCJ.BETA3           -0.07618  0.00008  -948.5533   0.0000
D:CALDCJ.BETA4            0.004616  0.000477    9.6876   0.0000
D:CALDCJ.BETA5           -0.001104  0.000281   -3.9278   0.0001
D:CALDCJ.BETA6           -0.004387  0.00026  -16.8579   0.0000
*****

R-SQ. (ADJ.) = 0.9996  SE = 0.141225  MAE = 0.066027  DurbWat = 1.890
552 observations fitted for 0 missing val. of dep. var.
```

### Output for regression of the Y force versus $\beta$



## Model fitting results for: D:CALDCJ.ZFORCE

```

*****
Independent variable      coefficient std. error   t-value  sig.level
*****
D:CALDCJ.BETA1           -0.000615  0.000124   -4.9753   0.0000
D:CALDCJ.BETA2            0.077882  0.000096  808.8691   0.0000
D:CALDCJ.BETA3           -0.010828  0.000113  -95.9468   0.0000
D:CALDCJ.BETA4            0.007902  0.000668   11.6259   0.0000
D:CALDCJ.BETA5            0.000144  0.000394    0.3665   0.7142
D:CALDCJ.BETA6            0.003224  0.000365    8.8405   0.0000
*****

R-SQ. (ADJ.) = 0.9904 SE = 0.195035 MAE = 0.104437 DurbinWat = 1.670
552 observations fitted for 0 missing val. of dep. var.

```

Output for regression of the Z force versus  $\beta$ 

## Model fitting results for: D:CALDCJ.LMOMENT

```

*****
Independent variable      coefficient std. error   t-value  sig.level
*****
D:CALDCJ.BETA1           9.499886E-7 2.375743E-5    0.3999   0.6894
D:CALDCJ.BETA2           -0.000079 1.852153E-6  -42.3199   0.0000
D:CALDCJ.BETA3            0.000042 2.170917E-6   19.4581   0.0000
D:CALDCJ.BETA4           -0.00293  0.000013  -227.9309   0.0000
D:CALDCJ.BETA5           -0.000139 7.579527E-6  -18.3146   0.0000
D:CALDCJ.BETA6            0.000135 7.015431E-6   19.2479   0.0000
*****

R-SQ. (ADJ.) = 0.9895 SE = 0.003909 MAE = 0.002561 DurbinWat = 1.761
552 observations fitted for 0 missing val. of dep. var.

```

Output for regression of the L moment versus  $\beta$ 

## Model fitting results for: D:CALDCJ.MMOMENT

```

*****
Independent variable      coefficient std. error   t-value  sig.level
*****
D:CALDCJ.BETA1           -0.000017 3.840091E-6  -4.3890   0.0000
D:CALDCJ.BETA2           5.976916E-8 2.993773E-6    1.9964   0.0464
D:CALDCJ.BETA3           9.510969E-7 3.509016E-6    0.2712   0.7863
D:CALDCJ.BETA4            0.000004 0.000021    1.9486   0.0519
D:CALDCJ.BETA5           -0.000072 0.000012   -5.8719   0.0000
D:CALDCJ.BETA6           -0.004847 0.000011  -409.7731   0.0000
*****

R-SQ. (ADJ.) = 0.9376 SE = 0.006157 MAE = 0.002864 DurbinWat = 0.978
552 observations fitted for 0 missing val. of dep. var.

```

Output for regression of the M moment versus  $\beta$

## Model fitting results for: D:CALDCJ.NMOMENT

*****				
Independent variable	coefficient	std. error	t-value	sig.level
*****				
D:CALDCJ.BETA1	0.000014	2.925893E-6	4.8717	0.0000
D:CALDCJ.BETA2	-0.000017	2.281835E-6	-7.3351	0.0000
D:CALDCJ.BETA3	0.000064	2.67455E-6	23.9685	0.0000
D:CALDCJ.BETA4	0.000087	0.000016	5.4789	0.0000
D:CALDCJ.BETA5	0.004763	9.337907E-6	510.0590	0.0000
D:CALDCJ.BETA6	0.000035	8.642946E-6	5.7551	0.0000
*****				
R-SQ. (ADJ.) = 0.9986 SE = 0.004693 MAE = 0.003297 DurbinWat = 0.498				
552 observations fitted for 0 missing val. of dep. var.				

Output for regression of the N moment versus  $\beta$ 

Output from multiple linear regression carried out by STATGRAPHICS on the calibration results of the sting in position 2.

## Model fitting results for: E:RCAL.XFORCE

*****				
Independent variable	coefficient	std. error	t-value	sig.level
*****				
E:RCAL.BETA1	-0.043476	0.000071	-610.9672	0.0000
E:RCAL.BETA2	0.001627	0.000067	24.2503	0.0000
E:RCAL.BETA3	0.001097	0.000056	19.4736	0.0000
E:RCAL.BETA4	0.001649	0.000386	4.0177	0.0001
E:RCAL.BETA5	0.002251	0.000214	10.5196	0.0000
E:RCAL.BETA6	-0.003134	0.00022	-14.2260	0.0000
*****				
R-SQ. (ADJ.) = 0.9985 SE = 0.113660 MAE = 0.077858 DurbinWat = 1.412				
552 observations fitted for 0 missing val. of dep. var.				

Output for regression of the X force versus  $\beta$

## Model fitting results for: E:RCAL.YFORCE

Independent variable	coefficient	std. error	t-value	sig.level
E:RCAL.BETA1	-0.000148	0.000201	-0.7384	0.4606
E:RCAL.BETA2	0.080851	0.000189	427.2701	0.0000
E:RCAL.BETA3	-0.008014	0.000159	-50.4424	0.0000
E:RCAL.BETA4	0.008251	0.001087	7.5585	0.0000
E:RCAL.BETA5	0.006539	0.000603	11.0042	0.0000
E:RCAL.BETA6	-0.002155	0.000621	-3.4583	0.0005

R-SQ. (ADJ.) = 0.9981 SE = 0.320535 MAE = 0.244482 DurbinWat = 0.193  
552 observations fitted for 0 missing val. of dep. var.

Output for regression of the Y force versus  $\beta$ 

## Model fitting results for: E:RCAL.ZFORCE

Independent variable	coefficient	std. error	t-value	sig.level
E:RCAL.BETA1	-0.00065	0.000048	-13.4858	0.0000
E:RCAL.BETA2	-0.007446	0.000045	-163.9369	0.0000
E:RCAL.BETA3	0.075455	0.000038	1978.5131	0.0000
E:RCAL.BETA4	-0.005081	0.000261	-19.4692	0.0000
E:RCAL.BETA5	-0.000531	0.000145	-3.6637	0.0003
E:RCAL.BETA6	0.005803	0.000149	38.9069	0.0000

R-SQ. (ADJ.) = 0.9999 SE = 0.076942 MAE = 0.059260 DurbinWat = 1.600  
552 observations fitted for 0 missing val. of dep. var.

Output for regression of the Z force versus  $\beta$ 

## Model fitting results for: E:RCALLMOMENT

Independent variable	coefficient	std. error	t-value	sig.level
E:RCAL.BETA1	-6.373111E-7	1.724264E-6	-0.3696	0.7118
E:RCAL.BETA2	0.000072	1.625878E-6	44.1874	0.0000
E:RCAL.BETA3	0.000151	1.365115E-6	110.2600	0.0000
E:RCAL.BETA4	-0.002952	9.341449E-6	-315.9922	0.0000
E:RCAL.BETA5	-0.000098	5.133891E-6	-19.8236	0.0000
E:RCAL.BETA6	0.000158	5.338435E-6	29.6448	0.0000

R-SQ. (ADJ.) = 0.9945 SE = 0.002754 MAE = 0.002046 DurbinWat = 1.577  
552 observations fitted for 0 missing val. of dep. var.

Output for regression of the L moment versus  $\beta$

## Model fitting results for: E:RCAL.MMOMENT

*****				
Independent variable	coefficient	std. error	t-value	sig.level
*****				
E:RCAL.BETA1	0.000045	1.603833E-6	28.3047	0.0000
E:RCAL.BETA2	5.407187E-7	1.512319E-6	0.3575	0.7208
E:RCAL.BETA3	8.610183E-6	1.260768E-6	6.7809	0.0000
E:RCAL.BETA4	0.000113	3.589994E-6	13.0019	0.0000
E:RCAL.BETA5	0.004755	4.821821E-6	986.7460	0.0000
E:RCAL.BETA6	0.000088	4.965571E-6	17.7122	0.0000
*****				
R-SQ (ADJ.) = 0.9996 SE = 0.002502 MAE = 0.001936 DurbWat = 1.699				
552 observations fitted for 0 missing val. of dep. var.				

Output for regression of the M moment versus  $\beta$ 

## Model fitting results for: E:RCAL.NMOMENT

*****				
Independent variable	coefficient	std. error	t-value	sig.level
*****				
E:RCAL.BETA1	0.000066	6.02726E-6	10.9186	0.0000
E:RCAL.BETA2	2.362947E-6	5.883346E-6	0.4158	0.6777
E:RCAL.BETA3	-0.00002	4.771834E-6	-4.2194	0.0000
E:RCAL.BETA4	-0.000092	0.000033	-2.8261	0.0049
E:RCAL.BETA5	-0.00002	0.000018	-1.1268	0.2603
E:RCAL.BETA6	0.004602	0.000019	246.8248	0.0000
*****				
R-SQ (ADJ.) = 0.9941 SE = 0.009027 MAE = 0.003719 DurbWat = 0.772				
552 observations fitted for 0 missing val. of dep. var.				

Output for regression of the N moment versus  $\beta$

Output from multiple linear regression carried out by STATGRAPHICS on the calibration results of the sling in position 2 after being repaired.

Model fitting results for: D:\CALSG.APX

```
*****
Independent variable      coefficient std. error   t-value  sig.level
*****
D:\CALSG.BETA_1          -0.043421  0.000064  -676.0153  0.0000
D:\CALSG.BETA_2           0.002771  0.000512    5.4082  0.0000
D:\CALSG.BETA_3           0.002477  0.000494    5.0164  0.0000
D:\CALSG.BETA_4           0.000461  0.000335    1.3778  0.1689
D:\CALSG.BETA_5           0.001929  0.000283    6.8061  0.0000
D:\CALSG.BETA_6          -0.002981  0.000259   -11.5667  0.0000
*****

R-SQ. (ADJ.) = 0.9990 SE = 0.148651 MAE = 0.063736 DurbinWat = 2.019
480 observations fitted for 0 missing val. of dep. var.
```

### Output for regression of the X force versus $\beta$

Model fitting results for: D:\CALSG.APY

```
*****
Independent variable      coefficient std. error   t-value  sig.level
*****
D:\CALSG.BETA_1          -0.000072  0.000167   -0.4299  0.5674
D:\CALSG.BETA_2           0.070135  0.001333   52.6263  0.0000
D:\CALSG.BETA_3          -0.005213  0.001285   -4.0577  0.0001
D:\CALSG.BETA_4           0.005333  0.000971    5.1219  0.0000
D:\CALSG.BETA_5          -0.001262  0.000737   -1.7120  0.0876
D:\CALSG.BETA_6           0.009355  0.00067   13.9564  0.0000
*****

R-SQ. (ADJ.) = 0.9973 SE = 0.386671 MAE = 0.289024 DurbinWat = 0.152
480 observations fitted for 0 missing val. of dep. var.
```

### Output for regression of the Y force versus $\beta$

## Model fitting results for: D:CALSG.APZ

```

*****
Independent variable      coefficient std. error   t-value sig.level
*****
D:CALSG.BETA_1           0.000231  0.000069    3.4105   0.0007
D:CALSG.BETA_2          -0.010285  0.000541   -18.0062   0.0000
D:CALSG.BETA_3           0.077193  0.000522   147.9874   0.0000
D:CALSG.BETA_4          -0.008185  0.000354   -17.4852   0.0000
D:CALSG.BETA_5           0.000397  0.000299    1.3272   0.1851
D:CALSG.BETA_6           0.002133  0.000272    7.8373   0.0000
*****

R-SQ. (ADJ.) = 0.9987 SE = 0.157007 MAE = 0.127341 DurbinWat = 0.385
480 observations fitted for 0 missing val. of dep. var.

```

Output for regression of the Z force versus  $\beta$ 

## Model fitting results for: D:CALSG.APL

```

*****
Independent variable      coefficient std. error   t-value sig.level
*****
D:CALSG.BETA_1           8.101039E-6 3.443863E-6    2.3523   0.0191
D:CALSG.BETA_2           0.000501  0.000027   18.2480   0.0000
D:CALSG.BETA_3          -0.000305  0.000026   -11.5134   0.0000
D:CALSG.BETA_4           0.005103  0.000018   284.1674   0.0000
D:CALSG.BETA_5           0.000139  0.000015    9.1434   0.0000
D:CALSG.BETA_6          -0.000372  0.000014   -26.9069   0.0000
*****

R-SQ. (ADJ.) = 0.9948 SE = 0.007970 MAE = 0.006576 DurbinWat = 1.355
480 observations fitted for 0 missing val. of dep. var.

```

Output for regression of the L moment versus  $\beta$ 

## Model fitting results for: D:CALSG.APM

```

*****
Independent variable      coefficient std. error   t-value sig.level
*****
D:CALSG.BETA_1           0.000036 5.25383E-6    4.5868   0.0000
D:CALSG.BETA_2          -0.000974  0.000062   -18.7019   0.0000
D:CALSG.BETA_3           0.007265  0.000005   144.7815   0.0000
D:CALSG.BETA_4          -0.000489  0.000034   -14.3383   0.0000
D:CALSG.BETA_5           0.004606  0.000029   159.8984   0.0000
D:CALSG.BETA_6           0.000663  0.000026    25.3159   0.0000
*****

R-SQ. (ADJ.) = 0.9957 SE = 0.015104 MAE = 0.011925 DurbinWat = 0.495
480 observations fitted for 0 missing val. of dep. var.

```

Output for regression of the M moment versus  $\beta$